DALTON

Reactions of $[S_2M(\mu\text{-}S)_2FeCl_2]^{2-}$ (M = Mo or W) with arenethiolate ions: influence of neighbouring metal sites on the rates and mechanisms of substitution at iron

Karin L. C. Grönberg, Richard A. Henderson* and Kay E. Oglieve

John Innes Centre, Nitrogen Fixation Laboratory, Norwich Research Park, Colney, Norwich NR4 7UH, UK

The kinetics of substitution of the chloro-groups in $[S_2Mo(\mu\text{-}S)_2FeCl_2]^{2-}$ by 4-$RC_6H_4S^-$ (R = Cl, H, Me or MeO) to form $[S_2Mo(\mu\text{-}S)_2Fe(SC_6H_4R\text{-}4)_2)^{2-}$ has been studied in MeCN using stopped-flow spectrophotometry. The mechanism involves initial binding of thiolate to Mo to generate $[S_2(4\text{-}RC_6H_4S)Mo(\mu\text{-}S)_2FeCl_2]^{3-}$, which has been detected by spectrophotometry and ^{1}H NMR spectroscopy. Subsequently, this species undergoes substitution of the chloro-groups on the neighbouring Fe by associative and dissociative pathways. The Mo–SC_6H_4R-4 residue affects these mechanisms in two ways: electron-withdrawing substituents facilitate the associative pathway (Hammett $\rho = +0.63$) whilst electron-releasing substituents facilitate the dissociative pathway ($\rho = -1.4$). Studies on the analogous clusters $[S_2W(\mu\text{-}S)_2FeCl_2]^{2-}$ and $[O_2Mo(\mu\text{-}S)_2FeCl_2]^{2-}$ indicated similar mechanisms.

Defining the mechanisms of substitution of iron–sulfur-based clusters contributes to our understanding of how the various components of a cluster affect their reactivity as a whole.[1] Previously we have shown that in cubane clusters containing the $\{MFe_3S_4\}$ (M = Mo or W) core the reactivity of the iron sites is affected by the heterometal.[2] The Fe atoms in these clusters behave as though they are more electron deficient than those in the analogous $\{Fe_4S_4\}^{2+}$ clusters. This is indicated by a change from a dissociative to an associative substitution mechanism.

The work reported in this paper concentrates on how the reactivity of iron sites is affected by changing the ligands bound to a neighbouring heterometal, M = Mo or W. This effect has been probed through studies on the substitution reactions of the binuclear species $[S_2M(\mu\text{-}S)_2FeCl_2]^{2-}$ (M = Mo or W) and $[O_2Mo(\mu\text{-}S)_2FeCl_2]^{2-}$ with 4-$RC_6H_4S^-$ (R = Cl, H, Me or MeO). These systems have the advantage that they contain only one Fe which can undergo substitution (Scheme 1). The work reported herein shows that thiolates bind initially to the Mo or W atom and thus the species which undergoes substitution is $[S_2(4\text{-}RC_6H_4S)M(\mu\text{-}S)_2FeCl_2]^{3-}$. By varying the thiolate the influence that ligands on M have on the reactivity of Fe can be investigated systematically.

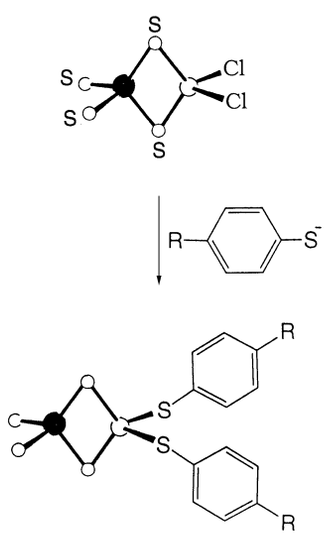

Scheme 1 ●, Mo or W; O, Fe

Experimental

All manipulations were routinely performed under an atmosphere of dinitrogen using Schlenk or syringe techniques as appropriate. Acetonitrile was distilled from CaH_2 immediately prior to use.

The complexes $[PPh_4]_2[S_2M(\mu\text{-}S)_2FeCl_2]$ (M = Mo or W)[3,4] were prepared by the literature methods, and $[PPh_4]_2[O_2Mo(\mu\text{-}S)_2FeCl_2]$ was prepared in an analogous fashion using $[NH_4][MoO_2S_2]$.[5] The salts $[NEt_4][SC_6H_4R\text{-}4]$ (R = Cl, H, Me or MeO) were prepared by a method analogous to that used for R = H and recrystallised from acetonitrile–diethyl ether mixtures.[6]

The ^{1}H NMR spectra were recorded on a JEOL GSX 270 spectrometer using CD_3CN as solvent. All chemical shifts are *versus* $SiMe_4$. The UV/VIS spectra were recorded on a Shimadzu PC 2101 spectrophotometer.

Kinetic studies

The kinetics were studied on a Hi-Tech SF-51 stopped-flow spectrophotometer, modified to handle air-sensitive materials.[7] The temperature was maintained at 25.0 °C using a Grant LE8 thermostat tank. The apparatus was interfaced to a Viglen 486 computer *via* an analogue to digital converter. Solutions were prepared under an atmosphere of dinitrogen and used within 1 h. All were transferred to the stopped-flow apparatus using gas-tight, all-glass syringes.

The kinetics were studied over the wavelength range $\lambda = 350$–570 nm, with most data collected at 500 nm. The rate constants calculated from the absorbance *vs.* time curves did not vary with the wavelength. At all wavelengths the reaction of $[S_2Mo(\mu\text{-}S)_2FeCl_2]^{2-}$ with 4-$RC_6H_4S^-$ shows a complicated absorbance *vs.* time curve. Fig. 1 shows the reaction with PhS^-: an initial absorbance decrease followed by an absorbance increase. These curves were fitted (using a computer program) to three exponentials: the first exponential corresponding to the absorbance decrease and the second and third to the absorbance increase.

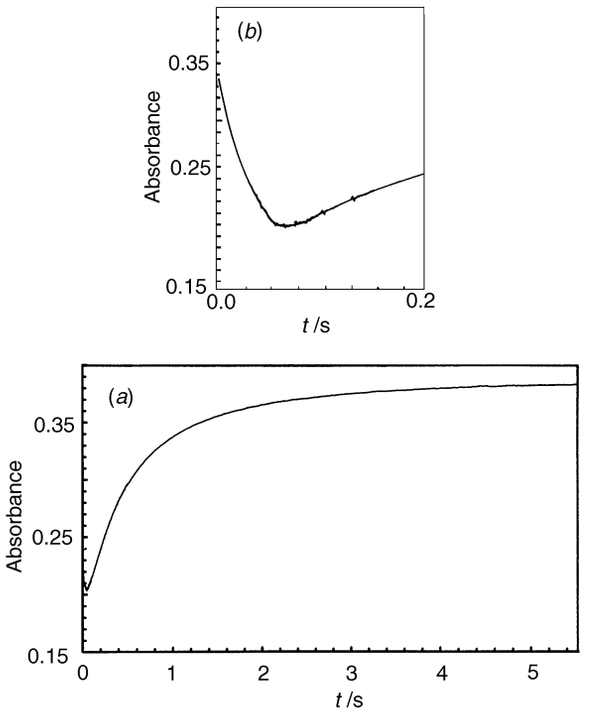

Fig. 1 (*a*) Stopped-flow absorbance *vs.* time curve for the reaction between $[S_2Mo(\mu\text{-}S)_2FeCl_2]^{2-}$ (1×10^{-4} mol dm^{-3}) and PhS^- (1.0 mmol dm^{-3}) in MeCN at 25.0 °C ($\lambda = 500$ nm). The entire trace was fit excellently by three exponentials: $A_t = 0.383 + 0.06\exp(-145t) - 0.093\exp(-3.5t) - 0.090\exp(-0.85t)$. (*b*) Expansion of the curve over 0–0.2 s, showing the initial absorbance decrease attributable to binding of PhS^- to Mo

The dependence of the reaction rate on the concentration of 4-$RC_6H_4S^-$ was established by the usual graphical methods[8] (Fig. 2).

Product analysis

The products of the reaction were identified as $[S_2M(\mu\text{-}S)_2Fe(SC_6H_4R\text{-}4)_2]^{2-}$ by ^{1}H NMR spectroscopy and subsequent comparison with the literature spectra (see Results and Discussion). Although the reactions were all complete within 20 s, it was observed that, over protracted times (*ca.* 20 min) and in the presence of an excess of thiolate, additional peaks attributable to $[Fe(SC_6H_4R\text{-}4)_4]^{2-}$ were observed. This is presumably due to some decomposition of $[S_2M(\mu\text{-}S)_2Fe(SC_6H_4R\text{-}4)_2]^{2-}$. For example, in the reaction of $[S_2M(\mu\text{-}S)_2FeCl_2]^{2-}$ with 4-$MeC_6H_4S^-$, $[Fe(SC_6H_4Me\text{-}4)_4]^{2-}$ was identified by ^{1}H NMR spectroscopy (see Fig. 5). An authentic sample of $[Fe(SC_6H_4Me\text{-}4)_4]^{2-}$ was generated *in situ* by the reaction of $FeCl_2$ (anhydrous) and an excess of $[NEt_4][SC_6H_4Me\text{-}4]$ in MeCN.

Results and Discussion

The reaction of $[S_2Mo(\mu\text{-}S)_2FeCl_2]^{2-}$ with an excess of 4-$RC_6H_4S^-$ (R = Cl, H, Me or MeO) in MeCN gives $[S_2Mo(\mu\text{-}S)_2Fe(SC_6H_4R\text{-}4)_2]^{2-}$ according to the stoichiometry in Scheme 1. Stopped-flow spectrophotometry reveals that this reaction is complicated; a typical absorbance *vs.* time curve is shown in Fig. 1. The reaction occurs in two distinct stages. Upon mixing 4-$RC_6H_4S^-$ and $[S_2Mo(\mu\text{-}S)_2FeCl_2]^{2-}$ there is an initial absorbance decrease which is followed by an absorbance increase. Analysis of the trace shows that it cannot be fitted by less than three exponentials: the initial absorbance decrease corresponds to one exponential and the increase to the following two. In addition, the latter two exponentials have approximately the same absorbance change. The rates of all three reactions increase linearly with the concentration of 4-$RC_6H_4S^-$, as illustrated in Fig. 2 for R = H.

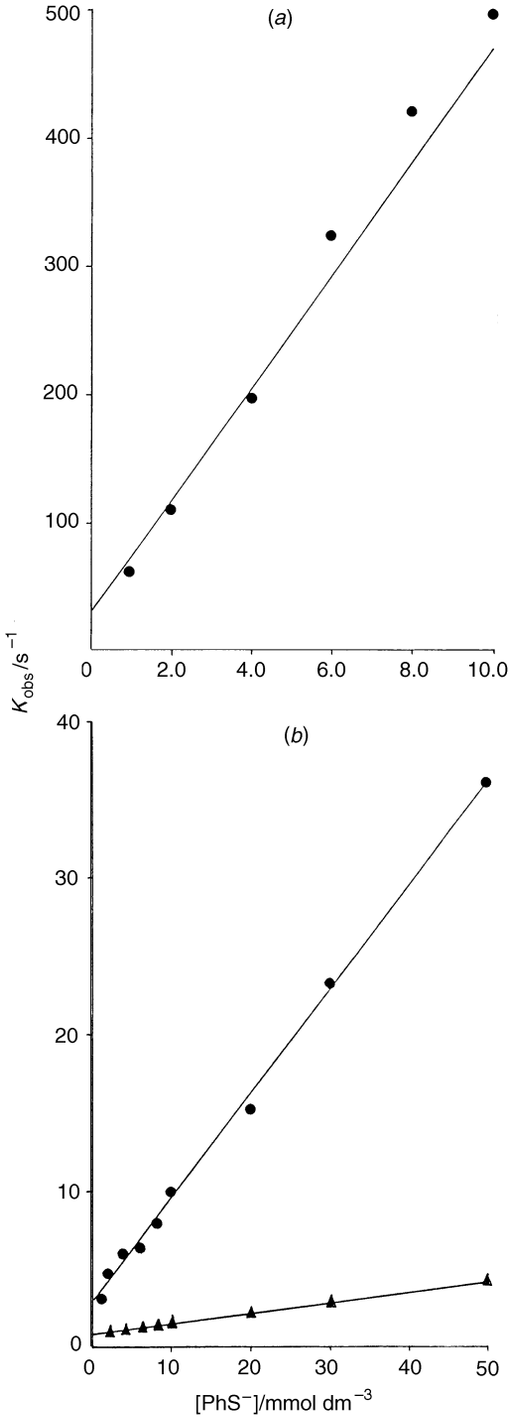

Fig. 2 (*a*) Dependence of k_{obs} on the concentration of PhS^- for the binding of PhS^- to $[S_2Mo(\mu\text{-}S)_2FeCl_2]^{2-}$ in MeCN at 25.0 °C ($\lambda = 500$ nm) corresponding to the initial absorbance decrease shown in Fig. 1. (*b*) Dependence of k_{obs} on the concentration of PhS^- for substitution of the two chloride ligands from $[S_2(PhS)Mo(\mu\text{-}S)_2FeCl_2]^{3-}$ (1×10^{-4} mol dm^{-3}): ●, first Cl; ▲, second Cl

This behaviour can be rationalised by a mechanism in which binding of 4-$RC_6H_4S^-$ to Mo (initial stage) is followed by substitution of the two chloro-groups on Fe (biphasic second stage). Scheme 2 shows the detailed pathways for the substitution of the first chloride. Substitution of the second chloride follows analogous pathways. We will now present the evidence for each step of this mechanism.

Initial stage: formation of $[S_2(4\text{-}RC_6H_4S)Mo(\mu\text{-}S)_2FeCl_2]^{3-}$

The initial absorbance decrease is attributable to the binding of 4-$RC_6H_4S^-$ to Mo. The kinetics observed shown in Fig. 2 and described by equation (1) is consistent with an equilibrium

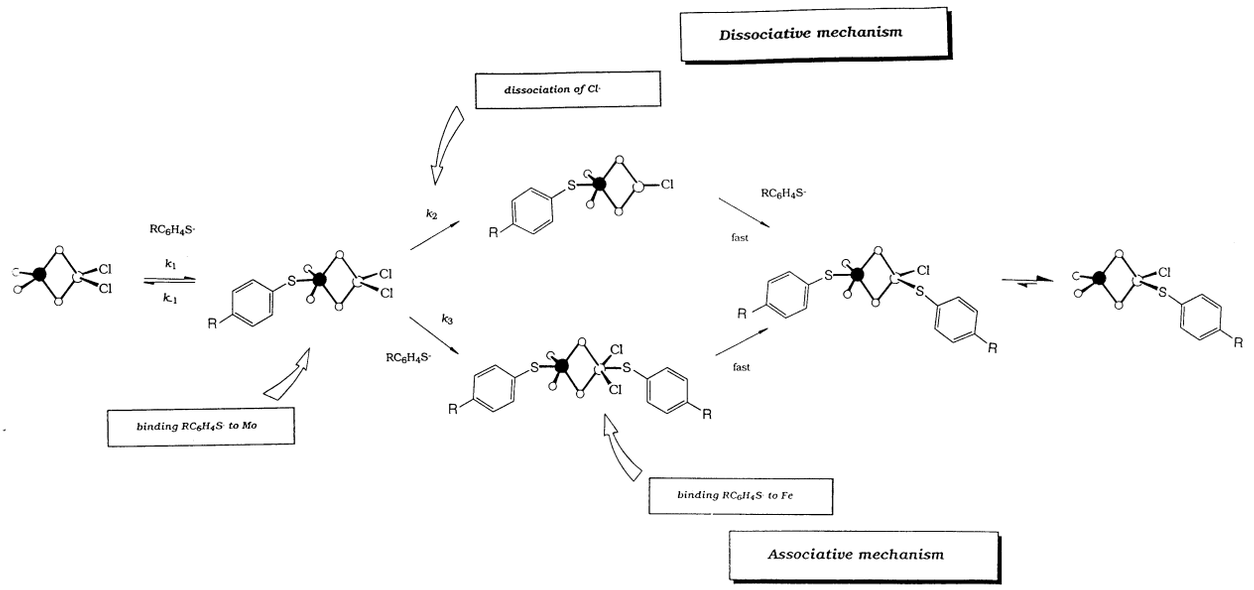

Scheme 2 Mechanism for substitution of the first chloro-group in $[S_2Mo(\mu\text{-}S)_2FeCl_2]^{2-}$ by 4-$RC_6H_4S^-$ in MeCN

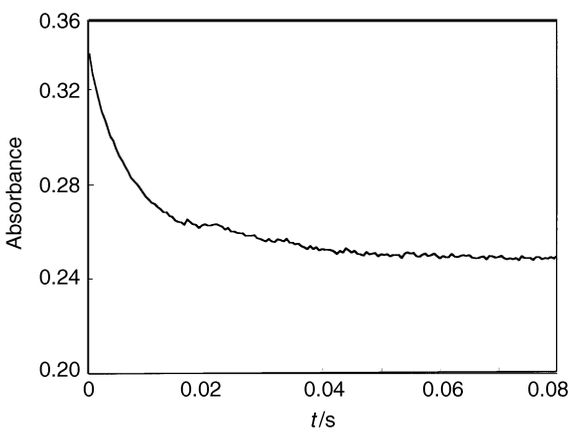

Fig. 3 Stopped-flow absorbance *vs.* time curve for the equilibrium binding of Cl^- (2.0 mmol dm^{-3}) to $[S_2Mo(\mu\text{-}S)_2FeCl_2]^{2-}$ (0.05 mmol dm^{-3}) in MeCN at 25.0 °C ($\lambda = 500$ nm). Trace fitted by the equation $A_t = 0.26 + 0.092\exp(-120t)$

$$-d[S_2Mo(\mu\text{-}S)_2FeCl_2^{2-}]/dt = (k_1^R[4\text{-}RC_6H_4S^-] + k_{-1}^R)[S_2Mo(\mu\text{-}S)_2FeCl_2^{2-}] \quad (1)$$

reaction.[9] Here and for the remainder of this paper the superscript R refers to the substituent on 4-$RC_6H_4S^-$. Analysis of the data gives $k_1^H = (2.0 \pm 0.1) \times 10^5$ dm^3 mol^{-1} s^{-1}, $k_{-1}^H = 70 \pm 10$ s^{-1} and the equilibrium constant $K_1^H = k_1^H/k_{-1}^H = (2.9 \pm 0.3) \times 10^3$ dm^3 mol^{-1}; $k_1^{Cl} = (8.0 \pm 0.2) \times 10^4$ dm^3 mol^{-1} s^{-1}, $k_{-1}^{Cl} = 40 \pm 6$ s^{-1} and $K_1^{Cl} = (2.0 \pm 0.3) \times 10^3$ dm^3 mol^{-1}.

For 4-$MeC_6H_4S^-$ and 4-$MeOC_6H_4S^-$ the binding to Mo is too fast to be measured by the stopped-flow technique even at the lowest concentration of thiolate used (0.5 mmol dm^{-3}). With these thiolates the half-life for the binding of 4-$RC_6H_4S^-$ to Mo must be shorter than the dead-time of the apparatus (2 ms) and hence $k_1^R > 7 \times 10^5$ dm^3 mol^{-1} s^{-1}. With these thiolates the absorbance *vs.* time traces consist of an initial absorbance decrease, complete within the dead-time of the apparatus, followed by a biphasic absorbance increase associated with substitution at Fe (see below). Similar behaviour is observed at high concentrations of PhS^- or 4-$ClC_6H_4S^-$, where the rate of binding of the thiolate to Mo exceeds that detectable by the stopped-flow apparatus.

Other anions such as Cl^- and CN^- apparently bind to Mo in an equilibrium reaction associated with an exponential absorbance decrease (Fig. 3). The kinetics exhibits the same two-term rate law as shown in equation (1), characteristic of an equilibrium reaction. For studies with Cl^-: $k_{1Cl} = (4.4 \pm 0.3) \times 10^4$ dm^3 mol^{-1} s^{-1}, $k_{-1Cl} = 30 \pm 5$ s^{-1}. For studies with CN^-: $k_{1CN} = (7.7 \pm 0.6) \times 10^4$ dm^3 mol^{-1} s^{-1}, $k_{-1CN} = 30 \pm 5$ s^{-1}.

It can be shown that Cl^- and PhS^- bind to the same site. In experiments where the concentration of PhS^- is kept constant and the concentration of Cl^- varied, the initial absorbance of the stopped-flow trace becomes progressively smaller until at high concentrations of Cl^- a relatively small absorbance change is observed, as indicated by the data in Table 1. If Cl^- and PhS^- competitively bind to Mo (Scheme 3) then in the absence of Cl^- the dominant species is $[S_2(PhS)MoS_2FeCl_2]^{3-}$, whilst at high concentrations of Cl^- the equilibria lie in favour of $[S_2(Cl)\text{-}MoS_2FeCl_2]^{3-}$. For the reactions shown in Scheme 3 the overall

Table 1 Spectrophotometric determination of K_0 for the equilibrium between $[S_2(PhS)Mo(\mu\text{-}S)_2FeCl_2]^{3-}$ and $[S_2ClMo(\mu\text{-}S)_2FeCl_2]^{3-}$

$[Cl^-]$/mmol dm^{-3}	Absorbance	10^5 x/mol dm^{-3}	K_0
0.0	0.60		
2.5	0.55	0.96	2.1
5.0	0.51	1.73	1.9
10.0	0.48	2.31	2.3
20.0	0.42	3.46	1.8
30.0	0.38	4.23	1.5
40.0	0.36	4.80	1.1
			mean 1.92

$[PhS^-] = 5.0$, $[S_2Mo(\mu\text{-}S)_2FeCl_2]^{2-} = 0.5$ mmol dm^{-3}; $x = [S_2ClMo(\mu\text{-}S)_2FeCl_2^{3-}]_{eq}$, $K_0 = [S_2(PhS)Mo(\mu\text{-}S)_2FeCl_2^{3-}]_{eq}[Cl^-]/[S_2ClMo(\mu\text{-}S)_2FeCl_2^{3-}]_{eq}[PhS^-]$. Molar absorption coefficients used: $\varepsilon_{PhS} = 1.2 \times 10^4$, $\varepsilon_{Cl} = 0.68 \times 10^4$ dm^3 mol^{-1} cm^{-1}.

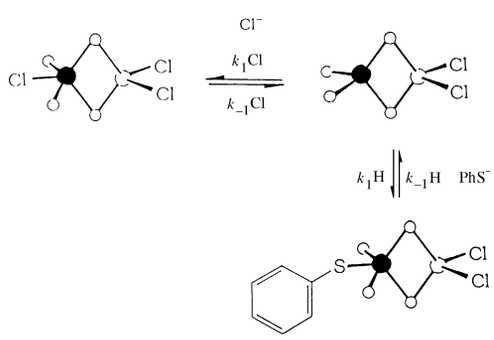

Scheme 3 Competitive binding of Cl^- and PhS^- to $[S_2Mo(\mu\text{-}S)_2\text{-}FeCl_2]^{2-}$ in MeCN

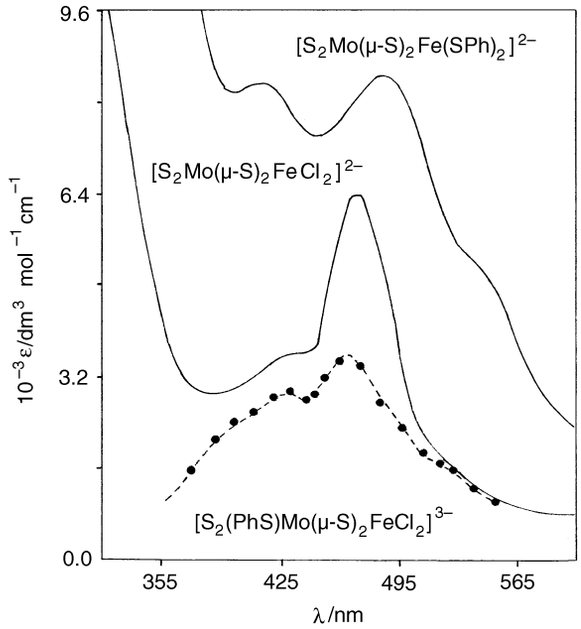

Fig. 4 Visible absorption spectra of $[S_2Mo(\mu\text{-}S)_2FeCl_2]^{2-}$, $[S_2Mo(\mu\text{-}S)_2Fe(SPh)_2]^{2-}$ and the intermediate $[S_2(PhS)Mo(\mu\text{-}S)_2FeCl_2]^{3-}$ (–●–), detected in the substitution reaction (see text)

equilibrium constant, $K_0 = [S_2(PhS)MoS_2FeCl_2^{3-}][Cl^-]/[S_2ClMoS_2FeCl_2^{3-}][PhS^-] = 1.92 \pm 0.3$ can be calculated from analysis of the spectrophotometric changes (shown in Table 1). In addition, since $K_0 = k_{-1Cl}k_1^H/k_{1Cl}k_{-1}^H$, the values of the elementary rate constants determined from the kinetic analyses can be used to give $K_0 = 1.95 \pm 0.3$, in excellent agreement with the value determined spectrophotometrically.

Since both Cl^- and PhS^- bind to $[S_2Mo(\mu\text{-}S)_2FeCl_2]^{2-}$ more rapidly than the Fe undergoes substitution, it seems likely that these ions bind to Mo initially. In addition the observation that substitution at Fe by the associative mechanism requires the addition of a further thiolate (see below) is difficult to rationalise if the initial PhS^- binds to Fe.

Two observations indicate that binding thiolate to Mo does not result in a 'dead-end' species but rather that substitution at Fe occurs *via* $[S_2(4\text{-}RC_6H_4S)Mo(\mu\text{-}S)_2FeCl_2]^{3-}$. First, at high concentrations of Cl^- ($[Cl^-]/[PhS^-] > 8$) where the cluster is predominantly $[S_2ClMo(\mu\text{-}S)_2FeCl_2]^{3-}$, substitution at Fe is faster than in the absence of Cl^-. Secondly, the rate of substitution at Fe by the dissociative pathway depends on the nature of the thiolate (see below).

The visible absorption spectrum of $[S_2(PhS)Mo(\mu\text{-}S)_2FeCl_2]^{3-}$ was determined in the range $\lambda = 360$–550 nm (Fig. 4) using stopped-flow spectrophotometry at the end of the first phase. This spectrum was recorded using $[S_2Mo(\mu\text{-}S)_2FeCl_2^{2-}] = 1 \times 10^{-4}$ mol dm^{-3} and $[PhS^-] = 5.0$ mmol dm^{-3}. Under these conditions 94% of the cluster is present as $[S_2(PhS)Mo(\mu\text{-}S)_2FeCl_2]^{3-}$ within the dead-time of the apparatus. This spectrum is very similar to that of $[S_2Mo(\mu\text{-}S)_2FeCl_2]^{2-}$ with a peak maximum at 472 nm, and shoulders at 425 and 520 nm. Such spectral characteristics are consistent with the visible absorption spectrum being dominated by S to Mo charge-transfer transitions associated with a 'MoS_4' chromophore.[10] The binding of PhS^- to Mo apparently does not cause a major perturbation to the energies of the electronic transitions.

Further evidence that thiolate binds initially to Mo comes from ^{1}H NMR spectroscopic studies (Fig. 5) on the reaction with 4-$MeC_6H_4S^-$. The choice of this thiolate is particularly advantageous because resonances at $\delta \approx 50$ (*Me*C_6H_4S–M; M = Fe or Mo) and ≈38 (*m*-H of MeC_6H_4S–M) are sufficiently paramagnetically shifted to not interfere with the signals of $[NEt_4]^+$ or free 4-$MeC_6H_4S^-$. In studies at low concentrations of 4-$MeC_6H_4S^-$, when $[4\text{-}MeC_6H_4S^-]/[S_2Mo(\mu\text{-}S)_2FeCl_2^{2-}] = 2.0$, three sets of paramagnetically shifted resonances in the region associated with Fe–SC_6H_4Me-4 are observed at δ 51.1, 50.5, 49.7 (Me) and 38.3, 37.4, 36.8 (*m*-H) respectively. In addition, a further resonances at δ 55.0, 52.9 and 29.8 are evident. Increasing the proportion of 4-$MeC_6H_4S^-$ to $[4\text{-}MeC_6H_4S^-]/[S_2Mo(\mu\text{-}S)_2FeCl_2^{2-}] = 4.0$ results in only two sets of signals attributable to Fe–SC_6H_4Me-4: δ 51.1, 50.1 (Me) and 37.7, 35.1 (*m*-H). The resonances at δ 55.0 and 29.8 are no longer evident. At still higher concentrations when $[4\text{-}MeC_6H_4S^-]/[S_2Mo(\mu\text{-}S)_2FeCl_2^{2-}] \geqslant 6.0$ the spectrum simplifies to that of authentic $[S_2Mo(\mu\text{-}S)_2Fe(SC_6H_4Me\text{-}4)_2]^{2-}$, consisting of resonances at δ 50.5 and 37.4.[11]

Although all the species observed in these experiments cannot be identified unambiguously, it seems likely that when $[4\text{-}MeC_6H_4S^-]/[S_2Mo(\mu\text{-}S)_2FeCl_2^{2-}] = 2.0$ the predominant solution species are $[S_2(4\text{-}MeC_6H_4S)Mo(\mu\text{-}S)_2FeCl_2]^{3-}$, $[S_2(4\text{-}MeC_6H_4S)Mo(\mu\text{-}S)_2FeCl(SC_6H_4Me\text{-}4)]^{3-}$, $[S_2Mo(\mu\text{-}S)_2FeCl(SC_6H_4Me\text{-}4)]^{2-}$ and $[S_2Mo(\mu\text{-}S)_2Fe(SC_6H_4Me\text{-}4)_2]^{2-}$. The last three account for the three sets of resonances attributable to Fe–SC_6H_4Me-4. Indeed, the resonances attributable to $[S_2Mo(\mu\text{-}S)_2Fe(SC_6H_4Me\text{-}4)_2]^{2-}$ (the one species for which we know the ^{1}H NMR spectrum) at δ 50.5 and 37.4 are clearly identifiable. Those at δ 55, 52.9 and 29.8 are assigned tentatively to the Mo–SC_6H_4Me-4 ligand in the first two of the solution species $[S_2(4\text{-}MeC_6H_4S)Mo(\mu\text{-}S)_2FeCl_2]^{3-}$ and $[S_2(4\text{-}MeC_6H_4S)Mo(\mu\text{-}S)_2FeCl(SC_6H_4Me\text{-}4)]^{3-}$

Formation of $[S_2(4\text{-}RC_6H_4S)Mo(\mu\text{-}S)_2Fe(SC_6H_4R\text{-}4)Cl]^{3-}$

After binding 4-$RC_6H_4S^-$ to Mo, the chloro-groups of Fe undergo substitution in a reaction associated with an absorbance increase where the final absorbance is that of $[S_2Mo(\mu\text{-}S)_2Fe(SC_6H_4R\text{-}4)_2]^{2-}$. Consistent with the sequential substitution of both chloro-groups this portion of the trace can only be simulated adequately by two exponentials. Both exponentials exhibit a dependence on the concentration of thiolate as defined by equation (2). In the first instance the discussion will

$$-d[S_2Mo(\mu\text{-}S)_2FeCl_2^{2-}]/dt = (k_2^R + k_3^R[4\text{-}RC_6H_4S^-])[S_2Mo(\mu\text{-}S)_2FeCl_2^{2-}] \quad (2)$$

focus on the substitution of the first chloro-group. The values of k_2^R and k_3^R are listed in Table 2. The kinetics of the second substitution will be discussed in a later section.

The two-term rate law (2) is consistent with the substitution being either an equilibrium reaction or occurring by a mixture of dissociative and associative mechanisms. These substitutions are not equilibrium reactions since the magnitude of the absorbance change for this stage does not vary with the concentration of 4-$RC_6H_4S^-$. Thus the k_2^R term in this rate law corresponds to a dissociative pathway involving rate-limiting dissociation of chloride from Fe, followed by rapid attack of 4-$RC_6H_4S^-$ at the, thus generated, vacant site. The k_3^R term corresponds to the associative pathway in which binding of 4-$RC_6H_4S^-$ to Fe occurs before, or concomitant with, dissociation of the chloro-group. Both associative and dissociative mechanisms for substitution are commonly observed with a variety of iron–sulfur-based clusters,[2,12] and with $[S_2Mo(\mu\text{-}S)_2FeCl_2]^{2-}$ both pathways operate in the reactions with a variety of thiolates.

By varying 4-$RC_6H_4S^-$ the electronic effect of the R substituent on the rate of substitution can be investigated. This is shown in the Hammett plot[13] in Fig. 6. There are three features of this Figure worthy of note: (1) $\log_{10}(k_2^R)$ and $\log_{10}(k_3^R)$ show reasonable linear correlations with Hammett σ_p constants; (2) the rate of the associative and dissociative pathways are affected differently by R (for the dissociative pathway, Hammett $\rho = -1.4$ and for the associative pathway, Hammett $\rho = 0.63$); (3) the dissociative pathway, k_2^R, exhibits a dependence on R. Feature (3) is mechanistically significant. In a dissociative mechanism attack of 4-$RC_6H_4S^-$ occurs after the rate-

Table 2 Summary of elementary rate constants for the substitution of $[Y_2(4\text{-}RC_6H_4S)M(\mu\text{-}S)_2FeCl_2]^{3-}$ (R = Cl, H, Me or MeO; Y = O, M = Mo; Y = S, M = Mo or W) at 25.0 °C in MeCN

		First substitution		Second substitution	
Cluster	R	k_2^R/s^{-1}	k_3^R/dm^3 mol^{-1} s^{-1}	$(k_2^R)'$/s^{-1}	$(k_3^R)'$/dm^3 mol^{-1} s^{-1}
$[S_2Mo(\mu\text{-}S)_2FeCl_2]^{2-}$	Cl	4.0 ± 0.3	(1.1 ± 0.1) × 10^3	1.9 ± 0.2	(1.9 ± 0.2) × 10^2
	H	3.0 ± 0.3	(6.4 ± 0.3) × 10^2	0.8 ± 0.1	84 ± 7
	Me	12.3 ± 1.0	(6.1 ± 0.3) × 10^2	1.7 ± 0.2	72 ± 7
	MeO	15.0 ± 1.0	(4.9 ± 0.3) × 10^2	1.5 ± 0.2	54 ± 6
$[O_2Mo(\mu\text{-}S)_2FeCl_2]^{2-}$	Cl		(4.3 ± 0.8) × 10^2		(1.6 ± 0.2) × 10^2
	H		(2.8 ± 0.3) × 10^2		66 ± 5
	Me		(3.4 ± 0.3) × 10^2		60 ± 5
	MeO		(3.0 ± 0.3) × 10^2		64 ± 5
$[S_2W(\mu\text{-}S)_2FeCl_2]^{2-}$	Cl	2.1 ± 0.2	(1.1 ± 0.1) × 10^3	0.29 ± 0.06	(7.1 ± 0.5) × 10^2
	H	0.35 ± 0.1	(1.7 ± 0.2) × 10^3	0.08 ± 0.006	(2.7 ± 0.3) × 10^2
	Me	2.2 ± 0.2	(7.0 ± 0.5) × 10^2	0.23 ± 0.05	(1.9 ± 0.3) × 10^2
	MeO	1.7 ± 0.2	(1.1 ± 0.1) × 10^3	0.07 ± 0.006	(3.1 ± 0.3) × 10^2

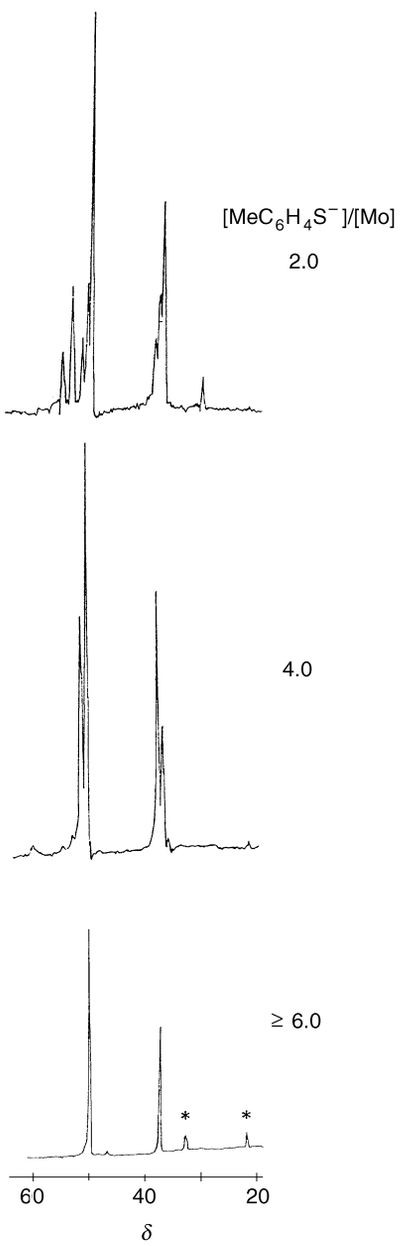

Fig. 5 Proton NMR spectra in the region δ +20 to +60 of mixtures of $[S_2Mo(\mu\text{-}S)_2FeCl_2]^{2-}$ and 4-$MeC_6H_4S^-$ in MeCN showing the resonances attributable to the Fe–SC_6H_4Me-4 residue and additional peaks at δ 55.0, 52.9 and 29.8 assigned to Mo–SC_6H_4Me-4. Peaks marked * in the bottom spectrum are those of $[Fe(SC_6H_4Me\text{-}4)_4]^{2-}$ produced by some decomposition (see Experimental section)

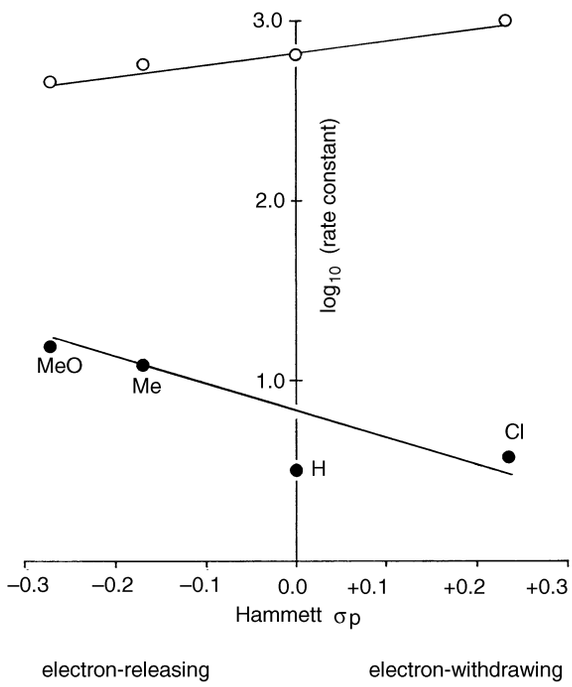

Fig. 6 Hammett plot of $\log_{10}(k_2^R)$ (dissociative mechanism, ●) or $\log_{10}(k_3^R)$ (associative mechanism, ○) against Hammett σ_p constant for the substitution of the first chloro-group in $[S_2Mo(\mu\text{-}S)_2FeCl_2]^{2-}$ with 4-$RC_6H_4S^-$ (R = Cl, H, Me or MeO)

limiting dissociation of chloride. Hence, the dependence of k_2^R on the nature of R must be a consequence of 4-$RC_6H_4S^-$ being bound to Mo. Electron-releasing ligands on Mo effectively increase the electron density at Fe, thus facilitating the dissociation of chloride. In contrast, electron-withdrawing ligands on Mo facilitate the associative mechanism by making the iron site more susceptible to nucleophilic attack. The associative mechanism will be discussed in more detail in a later section.

These studies show that for $[S_2Mo(\mu\text{-}S)_2FeCl_2]^{2-}$ the rate and mechanism of the substitution reaction at the neighbouring Fe depends on the ligands bound to Mo. Since the 4 substituent on Mo–SC_6H_4R-4 affects the dissociative and associative mechanisms differently the Hammett lines must cross. Fig. 6 shows that with a very electron-releasing ligand on Mo the reaction at Fe would occur exclusively by the dissociative mechanism, whilst a strongly electron-withdrawing substituent would effectively 'switch off' the dissociative, and facilitate the associative, mechanism.

A point which deserves further comment concerns the stage

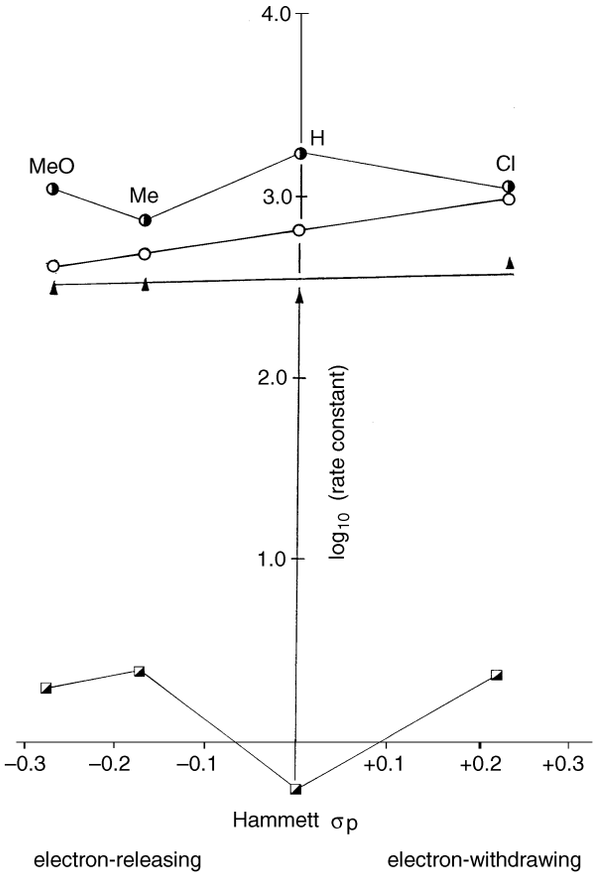

Fig. 7 Hammett plot for substitution of the first chloro-group by 4-$RC_6H_4S^-$ (R = Cl, H, Me or MeO) in: $[O_2Mo(\mu\text{-}S)_2FeCl_2]^{2-}$, associative mechanism (▲); $[S_2W(\mu\text{-}S)_2FeCl_2]^{2-}$, associative mechanism (◑), dissociative mechanism (◪). For comparison the data for the associative mechanism with $[S_2Mo(\mu\text{-}S)_2FeCl_2]^{2-}$ are shown (○)

at which the thiolate dissociates from Mo. Proton NMR spectroscopy shows that ultimately the product of the reaction is $[S_2Mo(\mu\text{-}S)_2Fe(SC_6H_4R\text{-}4)_2]^{2-}$. Clearly, upon substitution of the chloro-groups for thiolates the affinity of Mo for the thiolate must change sufficiently that this thiolate ligand is released. As discussed in this section, the thiolate bound to Mo affects the rate of substitution of the first chloride on Fe and thus we conclude that the thiolate remains bound to Mo until the first chloride has been substituted but, depending on the thiolate, may dissociate before the second substitution occurs (see next section).

Formation of $[S_2Mo(\mu\text{-}S)_2Fe(SC_6H_4R\text{-}4)_2]^{2-}$

The kinetics of substitution of the second chloro-group also occurs by the rate law (3), consistent with a mixture of associative and dissociative mechanisms. The values of $(k_2^R)'$ and $(k_3^R)'$ for the dissociative and associative substitution pathways (respectively) of the chloro-group in $[S_2(4\text{-}RC_6H_4S)Mo(\mu\text{-}S)_2Fe(SC_6H_4R\text{-}4)Cl]^{3-}$ are shown in Table 2.

$$-d[S_2Mo(\mu\text{-}S)_2FeCl_2^{2-}]/dt = \{(k_2^R)' + (k_3^R)'[4\text{-}RC_6H_4S^-]\}[S_2Mo(\mu\text{-}S)_2FeCl(SC_6H_4R\text{-}4)^{2-}] \quad (3)$$

The dissociative pathway (Hammett $\rho = +0.06$) is only slightly affected by the nature of the 4 substituent, whereas the associative pathway (Hammett $\rho = +1.0$) is facilitated by electron-withdrawing substituents. The small value of Hammett ρ for the dissociative pathway may indicate that, at least with most 4-$RC_6H_4S^-$, dissociation of thiolate from Mo occurs after the first substitution step and hence the only perturbing influence is the thiolate bound to Fe.

The associative mechanism

Thiolate plays two roles in the substitution of the first chloride by the associative mechanism (Scheme 2): as ligand to Mo and nucleophile to Fe. Electron-withdrawing R groups in the Mo–SC_6H_4R-4 residue decrease the electron density at Fe, making it more electrophilic and thus facilitating associative substitution. However, this same R group on free 4-$RC_6H_4S^-$ will diminish the nucleophilicity of this molecule. The net, observed effect on the associative mechanism is a combination of these two effects. The data presented in Fig. 6 indicate that the effect of the Mo–SC_6H_4R-4 residue dominates the reactivity of $[S_2Mo(\mu\text{-}S)_2FeCl_2]^{2-}$.

Two analogous systems have been studied: $[O_2Mo(\mu\text{-}S)_2FeCl_2]^{2-}$ and $[S_2W(\mu\text{-}S)_2FeCl_2]^{2-}$. Both show features similar to those of $[S_2Mo(\mu\text{-}S)_2FeCl_2]^{2-}$, indicating that analogous mechanisms operate.

Stopped-flow spectrophotometric studies on the reactions of $[O_2Mo(\mu\text{-}S)_2FeCl_2]^{2-}$ with 4-$RC_6H_4S^-$ show an initial absorbance decrease, complete within the dead-time of the apparatus, followed by a biphasic absorbance increase. This is consistent with the mechanism in which binding of 4-$RC_6H_4S^-$ to Mo is complete within 2 ms, followed by consecutive substitution of the two chloro-groups in $[O_2(4\text{-}RC_6H_4S)Mo(\mu\text{-}S)_2FeCl_2]^{3-}$. Analysis of the biphasic absorbance increase shows that the substitution of both chloro-groups exhibits a first order dependence on the concentration of 4-$RC_6H_4S^-$ and no thiolate-independent pathway, demonstrating an exclusively associative mechanism. Analysis of the data gives the values k_3^R and $(k_3^R)'$ for substitution of the first and second chloride respectively (Table 2).

The effect of the 4 substituent on the rate of the first substitution of $[O_2(4\text{-}RC_6H_4S)Mo(\mu\text{-}S)_2FeCl_2]^{3-}$ is illustrated in Fig. 7. The substituents have little effect on the rate of substitution by the associative pathway. However, since the stopped-flow absorbance *vs.* time trace is consistent with initial binding of 4-$RC_6H_4S^-$ to Mo, it seems likely that the electronic effects of the thiolate on Mo and as a nucleophile annul one another.

The substitution reactions of $[S_2W(\mu\text{-}S)_2FeCl_2]^{2-}$ exhibit similar stopped-flow absorbance *vs.* time traces. The rate laws for the substitution of the first and second chloro-groups are given by equations (2) and (3) respectively and the values of k_2^R, $(k_2^R)'$, k_3^R and $(k_3^R)'$ for substitution of both chloro-groups are shown in Table 2.

Analysis of the influence substituent R has on the rate of the first substitution of $[S_2W(\mu\text{-}S)_2FeCl_2]^{2-}$ (Fig. 7) shows that neither k_2^R nor k_3^R correlates well with Hammett σ_p. However, substituents which accelerate the associative mechanism inhibit the dissociative mechanism and *vice versa*. This behaviour is clearly related to that observed with the molybdenum analogue. It is not entirely clear why in this case the correlation over the entire range of thiolates is not linear. It would appear that the tungsten system is more sensitive to changes in the nature of the substituent R and whether the effect of the W-bound thiolate or the nucleophilic thiolate dominates the reactivity of the cluster varies through the series R = MeO, Me, H or Cl.

Conclusion

This study has shown how the rates of substitution of chloride ligands bound to an ion site are affected by changes to the coordination sphere of the neighbouring metal. Both the associative and dissociative mechanisms are affected by the ligands bound to Mo or W. A general feature that emerges is that electron-withdrawing ligands facilitate the associative mechanism but inhibit the dissociative pathway. This is most simply viewed as a consequence of the electron distribution at the iron site and the sensitivity of the dissociation of chloro-group to this feature. Further studies on similar systems to those described herein are essential to quantify the effects of a

variety of metal sites transmitting electron-density changes to neighbouring metals.

Acknowledgements

We thank the BBSRC for supporting this work and The John Innes Foundation for a studentship (to K. L. C. G.).

References

1 R. A. Henderson, *Nitrogen Fixation: Fundamentals and Applications*, Kluwer, Dordrecht, 1995, p. 117 and refs. therein.
2 R. A. Henderson and K. E. Oglieve, *J. Chem. Soc.*, *Dalton Trans.*, 1993, 1473 and refs. therein.
3 A. Müller, H. G. Tölle and H. Bögge, *Z. Anorg. Allg. Chem.*, 1980, **471**, 115.
4 D. Coucouvanis, E. D. Simhon, P. Stremple, M. Ryan, D. Swenson, N. C. Baenziger, A. Simopoulos, V. Papaefthymiou, A. Kostikas and V. Petrouleas, *Inorg. Chem.*, 1984, **23**, 741.
5 J. W. McDonald, G. D. Friesen, L. D. Rosenheim and W. E. Newton, *Inorg. Chim. Acta*, 1983, **72**, 205.
6 R. E. Palermo, P. P. Power and R. H. Holm, *Inorg. Chem.*, 1982, **21**, 173.
7 R. A. Henderson, *J. Chem. Soc.*, *Dalton Trans.*, 1982, 917.
8 J. H. Espenson, *Chemical Kinetics and Reaction Mechanisms*, McGraw-Hill, New York, 1981, p. 30.
9 R. G. Wilkins, *Kinetics and Mechanism of Reactions of Transition Metal Complexes*, VCH, Weinheim, 2nd edn., 1991, p. 32.
10 E. Diemann and A. Müller, *Coord. Chem. Rev.*, 1973, **10**, 79 and refs. therein.
11 R. G. Tieckelmann, H. C. Silvis, T. A. Kent, B. H. Huynh, J. V. Waszczak, B. K. Teo and B. A. Averill, *J. Am. Chem. Soc.*, 1980, **102**, 5550.
12 K. L. C. Grönberg and R. A. Henderson, *J. Chem. Soc.*, *Dalton Trans.*, 1996, 3667 and refs. therein.
13 Ref. 8, p. 195 and refs. therein.

Received 5*th November* 1996; *Paper* 6/07526F